Available online at www.sciencedirect.com

SciVerse ScienceDirect

Scripta Materialia 68 (2013) 777–780

Scripta MATERIALIA

www.elsevier.com/locate/scriptamat

Solid-solution copper alloys with high strength and high electrical conductivity

Kazunari Maki,* Yuki Ito, Hirotaka Matsunaga and Hiroyuki Mori

Mitsubishi Materials Corporation, Central Research Institute, 1975-2, Shimoishitokami, Kitamoto, Saitama 364-0022, Japan

Received 3 September 2012; revised 14 December 2012; accepted 18 December 2012
Available online 2 January 2013

Solid-solution copper alloys are standard and widely used conductive materials. However, it is generally considered difficult to significantly improve the balance between the strength and electrical conductivity of these alloys. Here, we designed copper alloys that exhibit high strength and conductivity by using solid-solution hardening enhanced by supersaturation with Mg. Cu–Mg alloy has a conductivity at least three times higher than that of the representative solid-solution Cu–Sn, while retaining comparable strength. Cu–Al–Mg alloy showed greater strength and conductivity than Cu–Sn.

Keywords: Copper alloys; Electrical resistivity/conductivity; Mechanical properties; Supersaturated solid-solution alloys

Copper alloys are widely used in industry as conductive materials in various electrical and electronic applications [1]. In particular, solid-solution (SS) copper alloys such as brass and phosphor bronze, despite having been developed long ago, are major workhorse materials because of their simple production processes, low cost, and adequate balance between mechanical strength and electrical conductivity (EC). To reduce the size and weight of the applications, copper alloys are often required to have high strength and high EC simultaneously, without loss of formability. However, conventional SS copper alloys are unable to meet these requirements because the solutes dissolved in copper cause a large decrease in EC with an increase in strength. Thus, it is widely recognized that significant improvements in the balance between strength and EC are difficult in SS copper alloys [2,3]. Therefore, very little attention has been paid to SS hardening for designing high-strength and high-EC copper alloys. For these requirements, the precipitation-hardening approach is often adopted for alloy design [2,3]. However, this approach is very expensive because it involves the use of additional production processes to generate large amounts of homogeneously distributed fine precipitates and/or use of expensive alloying elements such as Be, Ag, Ni, and Co [3]. Here, we have focused on an alloy design approach based on SS hardening enhanced by supersaturation. We used Mg as the alloying element, with an emphasis on its characteristics of a large linear size factor (14.7%), low atomic weight (24.3), high maximum solubility in Cu (~7 at.%), and a small increase in resistivity and a large increase in recrystallization temperature with alloying [4–6]. We have also considered the fact that Mg is one of the most abundant metallic elements on earth [7]. To date, several studies on the precipitation phenomenon in Cu–Mg alloys containing at least 3 at.% Mg have been reported [8–15]. However, there are no studies that focus on combining high strength and high EC through SS hardening enhanced by supersaturation with Mg. Here, by using this alloy design approach, we have developed copper alloys that exhibit high strength, high EC, and high heat resistance, while retaining favorable bend formability. These alloys include Cu–Mg and Cu–Al–Mg supersaturated SS alloys, prepared without any complicated production processes or expensive alloying elements.

In this work, Mg is added to Cu and light-weight Cu–15Al (at.%) to create SS alloys that exhibit high specific yield strength, or 0.2% yield strength (YS)/weight ratio, and 0.5-mm-thick cold-rolled (CR) specimens of Cu–xMg ($x = 3$, 4, 5, and 6 at.%) and Cu–15Al–3Mg are prepared as supersaturated SS alloys, since preliminary tests showed that the maximum values of x for obtaining supersaturated single-phase Cu–xMg and Cu–15Al–xMg were 6 and 3, respectively. The supersaturated Cu–xMg and Cu–15Al–3Mg are obtained easily by heating at 650–715 and 700–715 °C, respectively, above

* Corresponding author. Tel.: +81 48 593 0435; fax: +81 48 593 0436; e-mail: k-maki@mmc.co.jp

1359-6462
http://dx.doi.org/10.1016/j.scriptamat.2012.12.027

their solid-solubility curves and subsequent cooling at a rate high enough to suppress precipitation (e.g., water quenching). Pure Cu and conventional SS alloys of Cu–xMg ($x = 0.7$ and 2 at.%), Cu–xSn ($x = 0.4$, 1, 2, 3, and 5.6 at.%), Cu–xAl ($x = 4$, 8, 12, and 15 at.%), and Cu–xZn ($x = 8$, 13, 20, and 30 at.%) are also prepared to obtain comparative data. To evaluate and compare their characteristics, their recrystallized grain size and reduction ratio of final cold-rolling are fixed at ~40 μm and 75% (equivalent strain of 1.6), respectively, because the mechanical properties of metallic materials are significantly affected not only by the composition but also by the grain size and degree of cold working [1,16–20]. Some of the CR specimens were heat-treated at different temperatures of up to 600 °C for 1 h to investigate the influence of heat treatment (HT) on microstructure, mechanical properties, specific resistance (SR), and bend formability (See Supplementary material for experimental details).

Figure 1a–c shows the composition dependence of YS and tensile strength (TS), density, and SR, respectively, of the CR specimens. First, there is a significant increase in the YS and TS of Cu–Mg by Mg addition for the supersaturation range of 3–6 at.% Mg. Cu–6Mg shows a YS of 764 MPa and a TS of 781 MPa. Second, a comparison of Cu–15Al–3Mg and Cu–15Al data reveals that addition of 3 at.% Mg to Cu–15Al markedly enhances strength. The YS and TS of Cu–15Al–3Mg reach up to 908 MPa and 1.03 GPa, respectively. Third, the YS and TS increase in the order of Cu–Sn, Cu–Mg, Cu–Al, and Cu–Zn for alloys containing the same amount of additive elements, which is consistent with the sequence of their linear size factors [4]. Fourth, the yield ratio (YR), or YS/TS, of each alloy system decreases as its YS and TS increase. However, different alloy systems show different decreasing trends of the YR. Cu–6Mg and Cu–5.6Sn have high YR of 98% and 96%, respectively, which are almost identical to that of Cu (99%). Conversely, Cu–15Al–3Mg and Cu–15Al show relatively low YR of 88% and 83%, respectively. Figure 1b shows that addition of Mg and/or Al is very effective in reducing the density of copper alloy, which is in agreement with prediction based on their atomic weights. In contrast, there is little change in the density of Cu–Sn after Sn addition. The density values of Cu–6Mg and Cu–15Al–3Mg are 8.34 and 7.63 g/cm^3, respectively. These values are 7% and 15% lower than the density of Cu (8.93 g/cm^3), respectively. All the measured alloys exhibit an increase in SR as the amount of additive elements increases (Fig. 1c). However, Cu–Mg has a much lower SR than Cu–Sn and Cu–Al, which contain the same amount of additive elements. The SR values of Cu–6Mg and Cu–15Al–3Mg are 5.0×10^{-8} and 14.4×10^{-8} Ωm, respectively. Figure 1d shows the influence of HT on the mechanical properties of Cu–6Mg and Cu–15Al–3Mg. The YS and TS of Cu–15Al–3Mg are enhanced with HT at a low temperature of 200 °C for 1 h. This strength enhancement is very likely due to anneal hardening—observed when HT of a cold-worked SS copper alloy at 150–300 °C below the recrystallization temperature is accompanied by a small decrease in the SR [21,22]—because precipitates in the heat-treated Cu–15Al–3Mg are not observed by transmission electron microscopy (TEM). The low-temperature heat-treated Cu–15Al–3Mg has favorable mechanical properties, namely a YS of 1.02 GPa, a TS of 1.09 GPa, a specific YS of 134 k N m kg^{-1}, and a specific TS (TS/weight ratio) of 143 k N m kg^{-1}. In contrast, Cu–6Mg heat-treated at 200 °C shows almost no enhancement in the strength. HT of Cu–6Mg and Cu–15Al–3Mg at a high temperature of 400 °C for 1 h increases their uniform elongation; however, it also significantly decreases their strength. The high-temperature heat-treated Cu–6Mg and Cu–15Al–3Mg have YS of 435 and 614 MPa, respectively, which are 57% and 68% of those of the CR specimens, respectively.

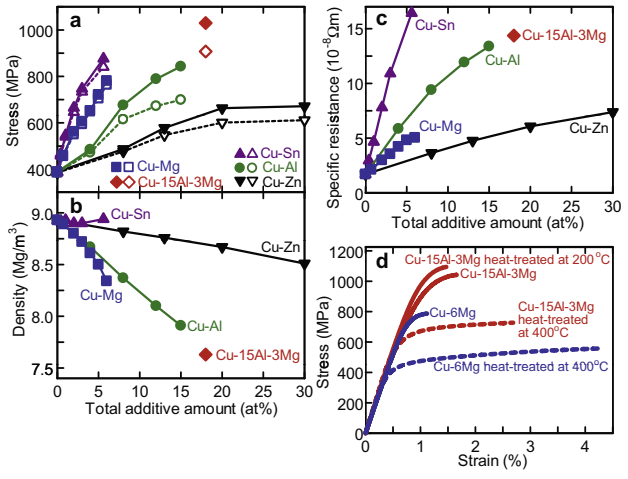

Figure 1. (a–c) Mechanical and physical properties of Cu–Mg, Cu–15Al–3Mg, Cu–Sn, Cu–Al, and Cu–Zn alloys: (a) 0.2% YS (open symbols), TS (solid symbols), (b) density, and (c) SR. (d) Influence of HT on stress-strain curves of Cu–6Mg and Cu–15Al–3Mg.

Figure 2 shows a compilation of the above results. First, supersaturated Cu–Mg and Cu–15Al–3Mg exhibit an excellent balance between YS and SR, owing to their high YS and low SR (Fig. 2a). This clearly differs from the general trade-off of SS alloys. Second, the difference from the general trade-off becomes clearer when plotting specific YS as a function of SR (Fig. 2b), since the specific YS of supersaturated Cu–Mg and Cu–15Al–3Mg are enhanced by both their high YS and low density (Fig. 1a and b). Third, in Cu–Mg, this difference becomes more apparent as the Mg content increases. There is clearly a major gap when Cu–6Mg is compared with Cu–5.6Sn, which has the highest specific YS among conventional SS alloys (Fig. 2b). Cu–6Mg and Cu–5.6Sn have similar specific YS of 92 and 94 k N m kg^{-1}, respectively, and different SR of 5.0×10^{-8} and 16.4×10^{-8} Ωm, respectively. Thus, Cu–6Mg exhibits a SR of less than one-third of that of Cu–5.6Sn (at least 3 times the EC of Cu–5.6Sn), while retaining a specific YS comparable to that of Cu–5.6Sn. Fourth, Cu–15Al–3Mg exhibits a remarkable specific YS of 119 k N m kg^{-1}. This is much higher than the specific YS of conventional SS alloys; Cu–15Al–3Mg has both a high YS of 908 MPa and a low density of 7.63 g/cm^3. The specific YS of Cu–15Al–3Mg is 27% higher than that of Cu–5.6Sn, and its SR of 14.4×10^{-8} Ωm is 12% lower than that of Cu–5.6Sn (Fig. 2b). Fifth, HT of Cu–15Al–3Mg at a low temperature of 200 °C in-

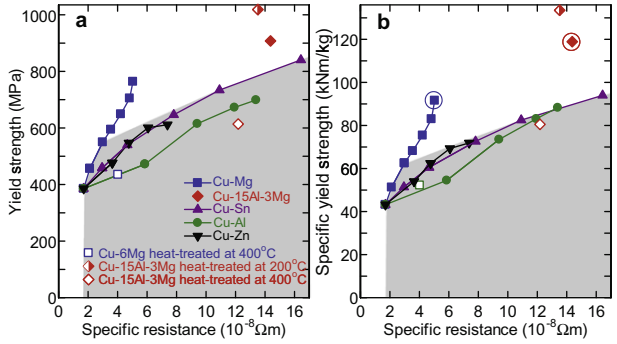

Figure 2. Mechanical properties of copper alloys as a function of SR: (a) YS and (b) specific YS. Experimental data for Cu and conventional SS alloys of Cu–xMg ($x = 0.7$, 2 at.%), Cu–xSn ($x = 0.4$, 1, 2, 3, 5.6 at.%), Cu–xAl ($x = 4$, 8, 12, 15 at.%), and Cu–xZn ($x = 8$, 13, 20, 30 at.%) are plotted in the shaded area. Data for supersaturated Cu–xMg ($x = 3$, 4, 5, 6 at.%) and Cu–15Al–3Mg show clear deviations from the general trade-off of SS alloys. In particular, Cu–6Mg and Cu–15Al–3Mg exhibit a clearly distinguishable balance between specific YS and SR (indicated within open circles). HT of Cu–15Al–3Mg at 200 °C enhances this balance. Conversely, HT of Cu–15Al–3Mg and Cu–6Mg at 400 °C severely degrades the balance.

creases the YS and specific YS to 1.02 GPa and 134 k N m kg^{-1}, respectively, and decreases the SR to 13.5×10^{-8} Ωm. Therefore, this HT at 200 °C further enhances the balance of Cu–15Al–3Mg between YS and SR or between specific YS and SR (Fig. 2a and b). Conversely, HT of Cu–15Al–3Mg and Cu–6Mg at a high temperature of 400 °C severely reduces their strengths as mentioned above. This markedly degrades the balance (Fig. 2).

As indicated in Figure 3a, the as-CR Cu–6Mg and Cu–15Al–3Mg possess a favorable bend formability, whereas Cu–6Mg and Cu–15Al–3Mg heat-treated at 400 °C have severely degraded bend formability despite larger uniform elongation relative to the as-CR alloys. Figure 3b and c shows TEM images of the as-CR alloys. Deformation twins and numerous dislocations were observed in both the as-CR alloys. In particular, a high density of deformation twins was found in Cu–15Al–3Mg, presumably because of its low stacking fault energy (SFE), as seen in the low SFE values of Cu–Al alloys [23]. As expected, no precipitates were formed in either alloy, implying that they are supersaturated SS. The TEM images (Fig. 3d and e) reveal that HT at 400 °C reduces the area with high dislocation density through recrystallization and forms many coarse precipitates with sizes of 50–200 nm. A high density of precipitates was observed at some grain boundaries (Fig. 3d and e). These precipitates in the heat-treated Cu–6Mg and Cu–15Al–3Mg are identified by electron diffraction and energy dispersive X-ray analysis as Cu_2Mg and Al-incorporated Cu_2Mg, respectively. These TEM observations are supported by the X-ray diffraction patterns scanned around the peak positions for (511) and (333) reflections of Cu_2Mg (see Fig. S1 in the Supplementary material). The patterns of the as-CR alloys reveal no detectable Cu_2Mg peaks, indicating that they are fully supersaturated. Conversely, the patterns of the heat-treated alloys show Cu_2Mg peaks. Based on the TEM images and previous reports of other metals

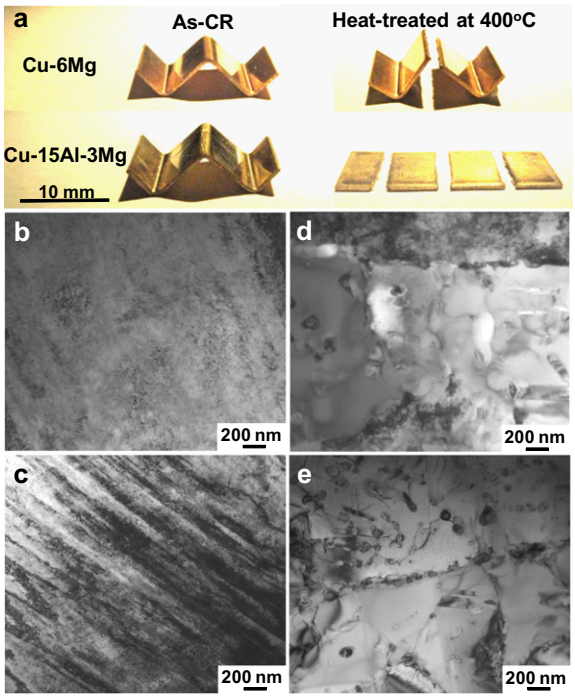

Figure 3. (a) Appearances of test specimens after 90° W-bending at a radius of 0.5 mm, with the bending axis perpendicular to the rolling direction. (b–e) TEM images of typical microstructures in (b) as-CR Cu–6Mg, (c) as-CR Cu–15Al–3Mg, (d) Cu–6Mg heat-treated at 400 °C for 1 h, and (e) Cu–15Al–3Mg heat-treated at 400 °C for 1 h. Precipitates are absent in as-CR (b) Cu–6Mg and (c) Cu–15Al–3Mg, indicating supersaturated SS. (d) Cu–6Mg and (e) Cu–15Al–3Mg heat-treated at 400 °C have many precipitates 50–200 nm in size, with some grain boundaries exhibiting a high density of such precipitates.

[24–27], there are two possible reasons for degradation of their bend formability after HT at 400 °C: (i) during bending, voids are formed around the coarse precipitates near the surface and cause crack initiation there; and (ii) many precipitates along boundaries act as crack initiation sites during bending, which leads to serious degradation of bend formability. This result, together with that shown in Figure 2, indicates that compared to precipitated Cu–6Mg and Cu–15Al–3Mg, the supersaturated Cu–6Mg and Cu–15Al–3Mg possess not only a remarkable balance between strength and EC but also superior bend formability.

Figure 4 shows changes in the Vickers microhardness and SR as a function of the isochronal HT temperature (1 h) for the CR specimens. First, the recrystallization temperature is greatly increased by Mg addition. Cu–2Mg is resistant to softening at temperatures up to 350 °C, whereas Cu, Cu–30Zn, Cu–15Al, and Cu–5.6Sn are rapidly softened owing to recrystallization by HT at 200, 300, 300, and 350 °C, respectively. That is, Cu–2Mg shows the highest softening temperature among the alloys, which indicates that Mg is a highly effective solute element for enhancing the heat resistance of copper alloys. Second, Cu–15Al–3Mg, Cu–15Al, and Cu–30Zn are hardened by HT in the temperature ranges of 100–350, 150–250, and 150–250 °C, respectively, most likely because of the anneal hardening described above. Anneal hardening of Cu–15Al–3Mg at high temperatures up to 350 °C may result from a combination of

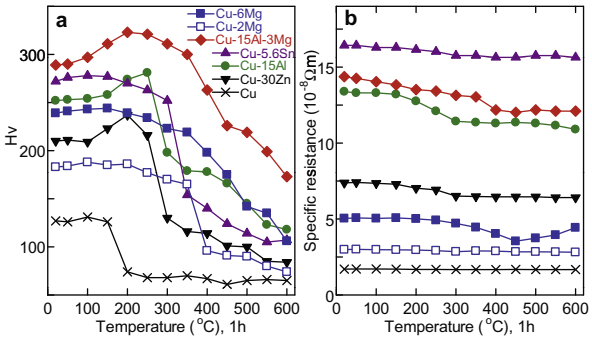

Figure 4. Changes in (a) Vickers microhardness and (b) SR as a function of isochronal HT (1 h) for Cu–6Mg and Cu–15Al–3Mg. For comparison, data for Cu, Cu–2Mg, Cu–5.6Sn, Cu–15Al, and Cu–30Zn are also plotted.

anneal hardening due to Al solute and the high softening temperature due to Mg solute. Third, Cu–6Mg and Cu–15Al–3Mg show superior heat resistance over conventional SS alloys. With regard to softening by HT at temperatures up to 350 °C, Cu–6Mg and Cu–15Al–3Mg show similar heat resistance to Cu–2Mg, indicating that there is little degradation of their microhardness with HT. Cu–6Mg and Cu–15Al–3Mg heat-treated at 350 °C show 90% and 93% of their highest Vickers microhardness values, respectively. In contrast, at temperatures higher than 350 °C, Cu–6Mg and Cu–15Al–3Mg show softening behaviors that differ from that of Cu–2Mg. They exhibit a fairly gradual decrease in the microhardness with increasing temperature as compared to Cu–2Mg, the microhardness of which rapidly decreases with HT at 400 °C. The reasons for the high heat resistance of Cu–6Mg and Cu–15Al–3Mg may be understood as follows. First, Mg solute inhibits softening at temperatures up to 350 °C. Second, HT at temperatures higher than 350 °C precipitates Cu_2Mg particles, as indicated by small decreases in the SR at the temperatures shown in Figure 4b. These particles restrict the motion of grain boundaries to retard recrystallization.

In summary, we have shown that supersaturation with Mg provides excellent performance for SS copper alloys, as represented by an enhancement of strength, heat resistance, and density reduction while retaining high EC. We designate the developed alloys—Cu–Mg and Cu–Al–Mg supersaturated with Mg—"magnesium bronze" and "aluminum-magnesium bronze", respectively. These bronzes are expected to be widely applicable to various conductive products of different shapes and sizes, as exemplified by sheets, strips, foils, bars, and wires, because they can be obtained using simple and commonly used production processes. Their mechanical and electrical characteristics can be tailored extensively by controlling the compositions and manufacturing conditions such as cold-working ratio, and HT temperature and time. Therefore, the developed bronzes, which combine superior performance and high manufacturability, show great promise as a next-generation workhorse conductive material.

We thank H. Chiba, T. Suzuki, Y. Dotani, T. Yamauchi, and A. Mitsuhashi for discussions.

Supplementary data associated with this article can be found, in the online version, at http://dx.doi.org/10.1016/j.scriptamat.2012.12.027.

[1] K. Lu, Science 328 (2010) 319.
[2] G. Ghosh, J. Miyake, M.E. Fine, JOM 49 (1997) 56–60.
[3] J.R. Davis (Ed.), ASM Specialty Handbook Copper and Copper Alloys, ASM International, Materials Park, OH, 2001, p. 3.
[4] H.W. King, J. Mater. Sci. 1 (1966) 79–90.
[5] C.A. Coughanowr, I. Ansara, R. Luoma, M. Hämäläinen, L. Lukas, Z. Metallkd. 82 (1991) 574–581.
[6] J.O. Linde, Helv. Phys. Acta 41 (1968) 1007–1015.
[7] M.M. Avedesian, H. Baker (Eds.), ASM Specialty Handbook Magnesium and Magnesium Alloys, ASM International, Materials Park, OH, 1999 (Preface).
[8] O. Dahl, Wiss Veroeff, Siemens-Konzern 6 (1927) 222–234.
[9] J. Wada, K. Nakamura, Rep. Inst. Sci. Technol. Univ. Tokyo 6 (1953) 313–315.
[10] H. Bohm, Z. Metallkd. 54 (1953) 142–146.
[11] T. Moisio, M. Mannerkoski, J. Inst. Met. 95 (1967) 268–272.
[12] S. Hori, S. Saji, T. Sekiya, J. Jpn. Copper Brass Res. Assoc. 19 (1980) 115–124.
[13] R. Chaim, J. Pelleg, M. Talianker, J. Mater. Sci. 22 (1987) 1609–1612.
[14] H. Tsubakino, R. Nozato, A. Yamamoto, Mater. Charact. 29 (1992) 7–13.
[15] K. Nishikawa, S. Semboshi, T.J. Konno, Solid State Phenom. 127 (2007) 103–108.
[16] E.O. Hall, Proc. Phys. Soc. B 64 (1951) 747–753.
[17] N.J. Petch, J. Iron Steel Inst. 174 (1953) 25–28.
[18] J.E. Bailey, P.B. Hirsch, Philos. Mag. 5 (1960) 485–497.
[19] M.A. Meyers, A. Mishra, D.J. Benson, Prog. Mater. Sci. 51 (2006) 427–556.
[20] K. Lu, L. Lu, S. Suresh, Science 324 (2009) 349–352.
[21] R.R. Hasiguti, J. Jpn. Inst. Met. 19 (1955) 103–106.
[22] J.M. Vitek, H. Warlimont, Metall. Trans. A 10A (1979) 1889–1892.
[23] A. Rohatgi, K.S. Vecchio, G.T. Gray III, Metall. Mater. Trans. A 32A (2001) 135–145.
[24] J. Sarkar, T.R.G. Kutty, D.S. Wilkinson, J.D. Embury, D.J. Lloyd, Mater. Sci. Eng. A 369 (2004) 258–266.
[25] M. Saga, M. Kikuchi, Y. Zhu, M. Matsuo, in: ICAA-6: Proc. sixth Int. Conf. on Aluminum Alloys, 1998, pp. 425–430.
[26] M. Asano, T. Minoda, Y. Ozeki, H. Yoshida, Mater. Sci. Forum 519–521 (2006) 771–776.
[27] A. Davidkov, R.H. Petrov, P.D. Smet, B. Schepers, L.A.I. Kestens, Mater. Sci. Eng. A 528 (2011) 7068–7076.